Article

Gas hydrate estimate in an area of deformation and high heat flow at the Chile Triple Junction

Lucía Villar-Muñoz[1,*], Iván Vargas-Cordero[2], Joaquim P. Bento[3], Umberta Tinivella[4], Francisco Fernandoy[2,5], Michela Giustiniani[4], Jan H. Behrmann[1] and Sergio Calderon-Diaz[2]

[1] GEOMAR Helmholtz Centre for Ocean Research, Wischhofstr. 1-3, 24148 Kiel, Germany.
[2] Universidad Andrés Bello (UNAB), Quillota 980, Viña del Mar, Chile.
[3] Escuela de Ciencias del Mar, Pontificia Universidad Católica de Valparaíso, Av. Altamirano 1480, Valparaíso, Chile.
[4] Istituto Nazionale di Oceanografia e di Geofisica Sperimentale (OGS), Borgo grotta gigante 42/c, 34010 Sgonico, Trieste, Italy.
[5] Centro de Investigación Para la Sustentabilidad (CIS), Universidad Andrés Bello, República 252, Santiago, Chile
* Correspondence: lucia.villar@gmail.com; Tel.: +56-9-5226-4461

Abstract: Large amounts of gas hydrate are present in marine sediments offshore Taitao Peninsula, near the Chile Triple Junction. Here, marine sediments on the forearc contain carbon that is converted to methane in a zone of very high heat flow and intense rock deformation above the downgoing oceanic spreading ridge separating the Nazca and Antarctic plates. This regime enables vigorous fluid migration. Here we present an analysis of the spatial distribution, concentration, estimate of gas phases (gas hydrate and free gas) and geothermal gradients in the accretionary prism and forearc sediments offshore Taitao (45.5° - 47° S). Velocity analysis of Seismic Profile RC2901-751 indicates gas hydrate concentration values <10% of the total rock volume, and extremely high geothermal gradients (<190 °Ckm^{-1}). Gas hydrates are located in shallow sediments (90-280 meters below the seafloor). The large amount of hydrate and free gas estimated (7.21x10^{11} m^3 and 4.1x10^{10} m^3, respectively), the high seismicity, the mechanically unstable nature of the sediments, and the anomalous geothermal conditions, set the stage for potential massive releases of methane to the ocean mainly through hydrate dissociation and/or migration directly to the seabed through faults. We conclude that the Chile Triple Junction is an important methane seepage area and should be the focus of novel geological and ecological research.

Keywords: BSR, gas hydrate, methane, seepage, active margin, Chile Triple Junction

1. Introduction

Gas hydrate is a crystalline ice-like solid formed by a mixture of water and gasses, mainly methane, giving place to clathrate structure [1,2] that can be stored in the pore space of marine sediments under low temperature (< 25°C) and high pressure (> 0.6 MPa) conditions. Methane gas may be produced biogenically at shallow depth, or may migrate from a deeper source through advective transport along pathways as fracture networks, faults or shear zones (e.g. 3). Since the gas hydrates are rich in methane, 1 m^3 of hydrate will yield 0.8 m^3 of water and 164 m^3 of methane at standard pressure and temperature (STP: 0°C, 0.101325 Mpa) conditions [4], significant amount of hydrate represents an unconventional and potential energy resources [5]. Moreover, gas hydrates play a part in the global climate change, geo-hazards and potential drilling hazards (e.g. [6-10]).

It is possible to identify gas hydrates in marine sediments by using seismic profiles. The main indicator is the so-called Bottom Simulating Reflector (BSR), whose presence is related to the impedance contrast between high velocity gas hydrate-bearing and the underlying low velocity free

gas layer [11-14]. Gas hydrate occurrences along the Chilean margin have been reported in many places by analysing the available seismic profiles (e.g., [11,14-27]) as well as more recently by direct identification of cold seeps emitting methane at the seafloor [28-34]. The first discovery of a seepage area was in 2004 offshore Concepcion. Afterwards, other bathyal seep sites were identified mainly by the presence of typical seep communities: a) off the Limari River at ~30°S (~1,000 m water depth); b) off El Quisco 33°S (~340 m water depth); c) off the Taitao Peninsula at ~46°S (~600 m water depth) [30-37].

Cold seeps sites are found in both active and passive margins and are related to the expulsion of methane-rich fluids. Chemosynthetic communities have been observed along active margins characterised by a well-developed accretionary prism, and also along tectonically erosive margins [38]. The Chile Triple Junction (CTJ) area is a spectacular example of tectonic erosion (e.g. [39]). Even though many investigations are associated to seepage identification and gas expulsion quantification (gas bubbles) (e.g. [29,38,40-42]), there are few cases where this is linked to estimate the size of the gas source, as gas hydrate and free gas [43].

Further, the studies that report estimates of gas hydrates concentrations along the Chilean margin are scarce, even if, in the last decades, gas phase concentrations have been estimated by fitting modelled velocity with theoretical velocity in absence of gas [44]. These estimates reach an average of 15% and 1% of total volume of gas hydrate and free gas concentrations, respectively [22,24,25,27]. A recent investigation of the southernmost Chilean continental margin shows that highly concentrated and regionally extensive methane hydrate reservoir is present in marine sediments [27]. This could be an important natural resource for Chile, but, by the way of hydrated decomposition, also potentially poses a great environmental threat.

On the other hand, the Chilean south-central margin is one of the tectonically most active regions on Earth, with very large and mega-scale earthquakes occurring every 130 and 300 yr, respectively [45]. The margin segment close to the CTJ is characterised by high seismicity [46,47] that may trigger submarine sediments sliding and eventual gas hydrate dissociation. Some authors suggest that large subduction zone earthquakes have the potential to trigger hydrocarbon seepage to the ocean and possibly the atmosphere (e.g., [29,48]). In this context, known gas hydrate quantities stored beneath of marine sediments play an important role in the geohazard assessment. Besides, in subduction zones as the Chilean margin, fluids play a key role in the nucleation and rupture propagation of earthquakes [49], and are a major agent of advective heat transfer from depth to the Earth's surface. For this reason, it is crucial to know the pathways where methane-rich fluids could migrate. The release of this methane stored in the forearc wedge could have consequences for the ocean and atmosphere systems, and the destabilized gas hydrate-bearing sediments are a formidable geohazard, in the form of submarine slumps, induced earthquakes, and tsunamis (e.g., [2,6,50-54]).

The particularity of the Chilean margin close to the CTJ, with anomalous heat flow and high seismicity, together with the presence of hydrothermal systems (e.g. [55]) and possible seafloor seeps offers a unique scenario to study hydrate deposits. The aim of this study is to characterize and estimate the methane concentrations (hydrate and free gas phases) stored in the marine sediments in order to understand the potential amount of this gas that could be released through these natural pathways, likely affecting the geochemical properties of the seawater and, consequently, the marine ecology.

1.1 Geological Setting

The CTJ (Fig. 1) is the site of the intersection of three tectonic plates: Nazca, Antarctic and South America [39,56,57]. Here, the Chile Rise (CR), an active spreading center, is being subducted beneath the South American continental margin. Ridge subduction began near Tierra de1 Fuego 14 million years ago (Ma) and, then, migrated northwards to its current position north of the Taitao Peninsula

(e.g. [15]). The Nazca plate subducts beneath South America in an ENE direction at a rate of about 80-90 mm/a north of the CTJ, and the Antarctic plate subducts in an ESE direction at about 20 mm/a south of the CTJ (e.g. [56]). The CR spreading rate has been estimated about 70 km/Ma over the past 5 Ma, but within the last 1 Ma it has slowed down to about 60 km/Ma (e.g. [58]).

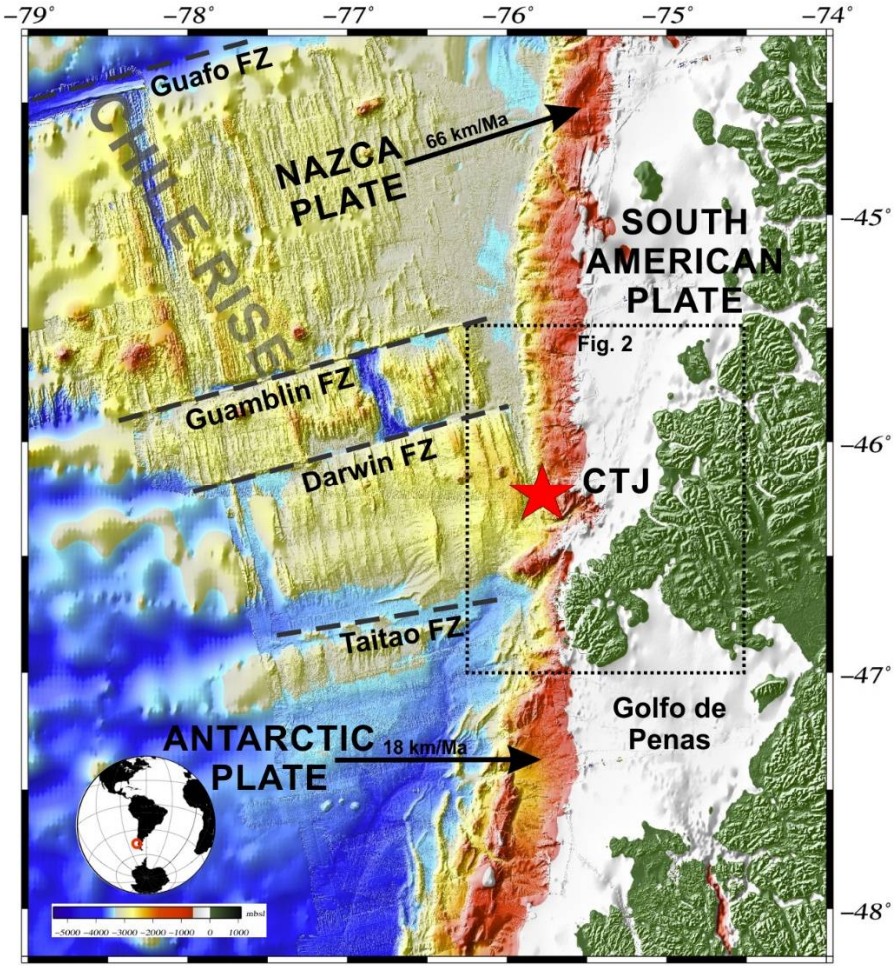

Figure 1. Location map of the study area offshore Taitao Peninsula. The bathymetry is based on GEBCO_08 Grid (version 20091120, http://www.gebco.net) and integrated with IFREMER grid (cruise of the R/V L'Atalante, 1997). Tectonic setting of the Nazca, Antarctic and South American plates: dashed black lines show the main Fracture Zones (FZ), red star marks a triple junction of the plates (CTJ) and dashed square correspond to Fig. 2.

Close to the CTJ, the gas hydrate environment has peculiar characteristics relative to hydrate occurrences elsewhere. In fact, the ridge-trench collision perturbs pressure and temperature (PT) conditions within the sediment where hydrates have formed [11]. Very high heat flow in excess of 250 mWm^{-2} is estimated above practically zero-age subducted crust (Fig. 2). This is based on heat flow values derived from the depth of gas hydrate bottom-simulating reflectors [26,59] and direct measurements during the last decades [57,60].

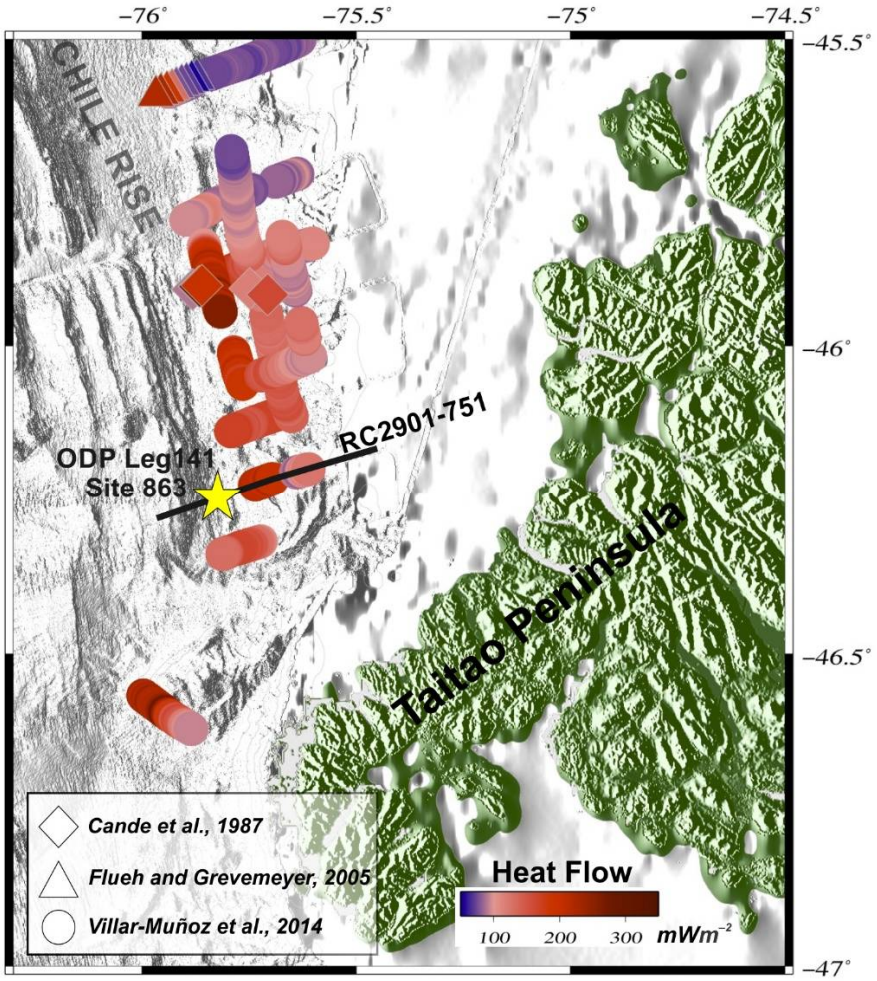

Figure 2. Heat flow (in mW m^{-2}) large-scale colour-coded based on BSR-derived heat flow and heat probes available for the area studied (after [26]). See text for description.

The BSR-derived heat flow values are in general agreement with probe and borehole measurements [61]. Besides, high temperature gradients of 80-100 °C/km were obtained at the toe of the continental wedge (e.g. Site 863 in Fig. 2), just above the subducted zero-age crust [55]. The thermal anomaly in the region varies rapidly due to the presence of a strong convective circulation [62].

More recently explorative work at the seafloor close to the CTJ has provided evidence for a sediment-hosted hydrothermal source near (~50 km) a methane-rich cold-seep area [63]. Advective methane transport operates within 5 km of the toe of the accretionary prism [59,64]. However, in the interior regions of the wedge, free gas migration and in situ gas production (within the hydrate stability region) build-up the hydrate [15], and BSR-depth towards trench appears to rise in the sediments in proximity of the spreading ridge [15,26].

Moreover, gas at the base of the hydrate layer at the CTJ could also be produced from hydrate dissociation when changes in PT conditions shift zone of hydrate stability upward not only due to accumulation of overburden, but also due to changes in PT conditions associated with active ridge subduction [11]. Increasing heat flow, associated with the approach of the CR, may have caused the base of the hydrate stability field to migrate ~300 m upwards in the sediments [15].

In this complex region, we find both active margin tectonic regimes: subduction erosion and subduction accretion occurring in close proximity (e.g., [65]). [66] assumes that the tectonic evolution of the Chile margin in the area reflects the evolution of the tectonic regime at depth: subduction

erosion from 5-5.3 to 1.5-1.6 Ma followed by subduction accretion since 1.5-1.6 Ma. [67] suspects that subduction accretion occurring today along the pre-subduction segment is linked to a dramatic post-glacial increase in trench sediment supply. From evidence found by drilling at Ocean Drilling Program (ODP) Site 863 (Fig. 2) at the CTJ proper, it was concluded that accretion ceased in late Pliocene, and presently the small frontal accretionary prism is undergoing tectonic erosion [39,55].

2. Materials and Methods

2.1 Database

Available seismic data were acquired in 1988 onboard R/V Robert Conrad. The seismic survey was carried out in the framework project entitled "Paleogene geomagnetic polarity timescale" for Empresa Nacional del Petroleo (ENAP). Seismic profiles were shot using an air gun array with a 3768 cu. The shot spacing was 50 m approximately. The length streamer was 3000 m and includes 236 channels spaced each 12.5 m. Seismic line RC2901-751 was analysed and modelled in this study, other profiles close to the CTJ were used to estimate hydrate phases.

During ODP Leg 141, the Site 863 (Fig. 2) were drilled along the profile RC2901-751 and is located few kilometers south of the CTJ, in an area where the axis of the spreading ridge subducted at 50 ka. Porosity and temperature data were obtained from this Site.

2.2 Methods

The processing was performed by using open source Seismic Unix software and codes ad-hoc [68] and includes a tested method reported in several studies [14,22,24,25,27,43,69]: a) BSR identification, b) seismic velocity modelling, c) gas-phases estimates and d) geothermal gradient estimation.

a) BSR identification: a stacking section was obtained by using a standard processing (i.e geometry arrangement, spherical divergence, normal moveout velocity analysis, stacking and filtering) in order to identify BSR. Once identified the BSR, a selected part was chosen to model the seismic velocity.

b) Seismic velocity modelling: to model the seismic velocity the Kirchhoff Pre-stack Depth migration (PreSDM) was computed. An iteratively layer stripping approach was performed, in which each layer was modelled in depth [70]. To correct the velocity an iterative migration velocity analysis was performed (to details see in [71]). In our case three layers were modelled. The first one between seawater level and seafloor reflector (SF layer), the second one between seafloor and BSR reflectors (BSR layer) and the third one between BSR and Base of Free Gas reflectors (BGR layer). The minimum error for SF, BSR and BGR layers was obtained after 4, 25 and 15 iterations, respectively. Below BGR layer a velocity gradient was included. In order to improve the final migration result, a smoothed velocity model was used. Finally, a band-pass filtering and mixing was applied on the final stacking section.

c) Gas-phases estimates: Once built the final velocity model, it was converted in gas-phase concentration model. A qualitative estimate can be obtained comparing the modelled velocity curves against theoretical curves in absence of gas, in which positive anomalies can be associated to gas hydrate presence, while negative anomalies are related to free gas presence. Finally, a quantitative estimate can be obtained by fitting the velocity model with a theoretical model and the result is a gas phase (gas hydrate and free gas) concentration model in terms of total volume (for more details see [44]).

Preprints (www.preprints.org) | NOT PEER-REVIEWED | Posted: 26 October 2018 doi:10.20944/preprints201810.0619.v1

Peer-reviewed version available at Geosciences 2019, 9, 28; doi:10.3390/geosciences9010028

d) Geothermal gradient estimation: The geothermal gradient can be estimated by using the following relation:

$$dT/dZ=(T_{BSR}-T_{SEA})/(Z_{BSR}-Z_{SEA}),$$

where seafloor and BSR depths (Z_{BSR}, Z_{SEA}) were extracted from seismic sections and seafloor and BSR temperatures (T_{BSR}, T_{SEA}) were taken from measurements reported by ODP leg 141 and the gas hydrate stability curve proposed by [4], respectively. Our estimation considers only methane because ethane gas concentration is negligible.

3. Results

3.1 BSR identification

From Kirchhoff PreSDM (Fig. 3), it is possible to recognize:

a) A normal fault at a distance of 7 km representing the boundary between lower and upper part. Moreover, evidence of slip affecting the seafloor, as shallow faults and fractures, is registered from 8 to 15 km of distance.

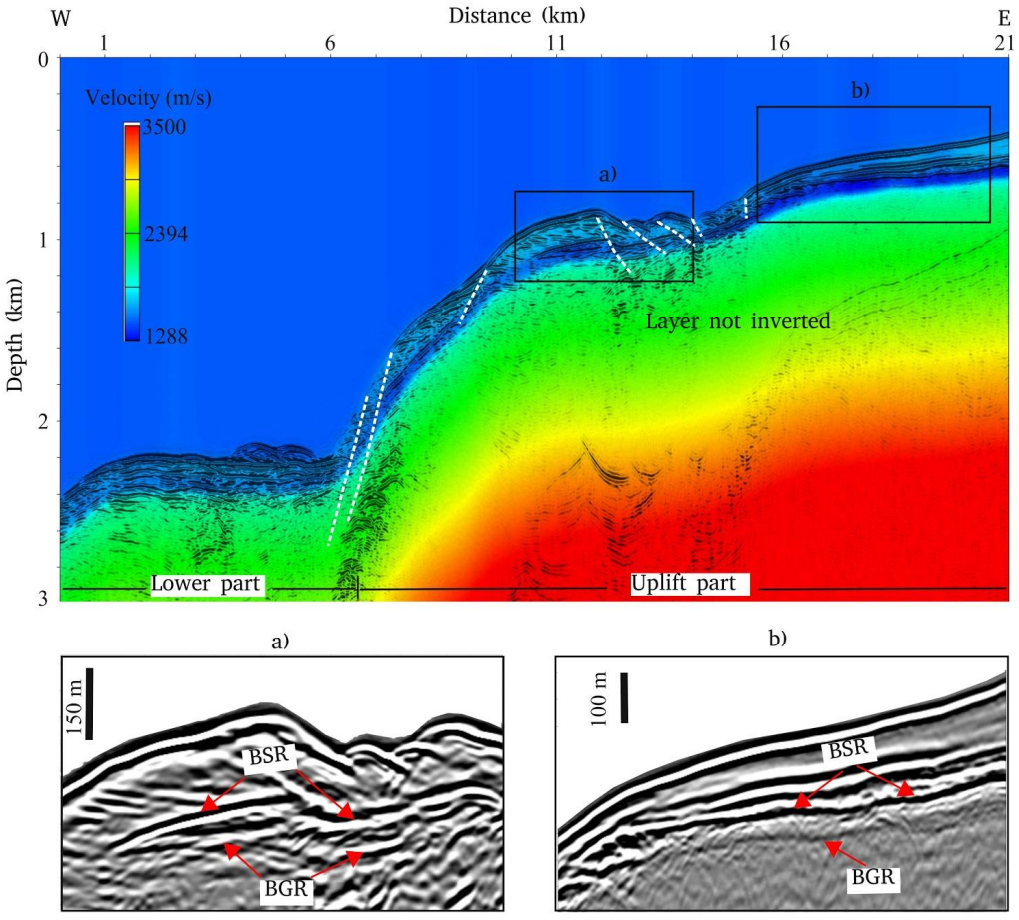

Figure 3. Velocity model superimposed to the Kirchhoff PreSDM section. The rectangles in the section indicate the position of the zooms in panel a and b, in which BSR and BGR (if present) are indicated by red arrows. Dotted lines indicate faults and fractures.

b) A strong and continuous BSR across the section, locally weak or null where faults and fractures appear. Below the BSR, it is possible to recognize a weak but continuous reflector interpreted as BGR and, so, a free gas layer with a thickness of about 70 m.

Preprints (www.preprints.org) | NOT PEER-REVIEWED | Posted: 26 October 2018 doi:10.20944/preprints201810.0619.v1

Peer-reviewed version available at Geosciences 2019, 9, 28; doi:10.3390/geosciences9010028

c) A variable depth of the BSR ranging between 80 and 150 meters below seafloor (mbsf). The maximum depth of BSR was detected at about 2200 mbsf from 0 to 6 km, while the minimum depth (about 80 mbsf) was identified upwards (from 7 to 16 km). From 16 to 21 km of distance, where the water column is limited, the BSR depth increases reaching a depth of 150 mbsf.

3.2 Seismic velocity model

Above the BSR it was identified a velocity layer with velocity values ranging from 1650 to 1740 m/s, while below it a variable low velocity layer was recognized (from 1288 to 1550 m/s). Below the BSR the velocity decreases upwards reaching its minimum value from 15 to 21 km of distance (Fig. 3). An opposite velocity trend was observed above the BSR; in fact, when the velocity increases above the BSR (from 10 to 21 km of distance), the minimum velocity values are found below it.

3.3 Gas phases estimates

High gas hydrates concentrations area located from 7 to 14 km of distance at 1000 m water depth approximately, reaching values ranging between 7 and 10% of total volume. Low gas hydrates concentrations (with values from 1 to 3 % of total volume) are detected from 1 to 6 km of distance at 2200 m water depth and from 15 to 20 km of distance at 600 m water depth (Fig. 4). In the portion of shallow water (from 15 to 20 km of distance) high free gas concentrations are present with values up to 0.8% of total volume. Note that a gas-phases (hydrate and free gas) concentrations show an opposite trend. In fact, high gas hydrate concentrations overlay low free gas concentrations, while high free gas concentrations underlay low gas hydrate concentrations (see Fig. 4; from 7 to 14 km and 15 to 20 km of distance respectively).

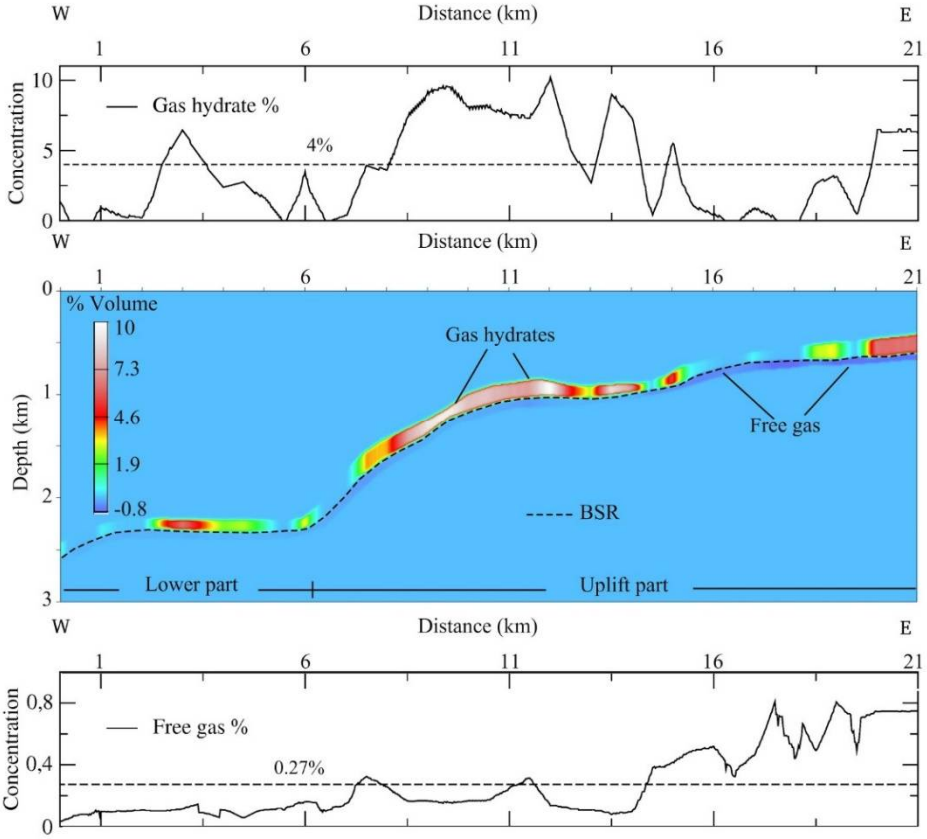

Figure 4. Gas phase concentrations model and profiles relative to RC2901-751 seismic profile. *Top panel*: gas hydrate concentration values. *Middle panel*: gas phase concentration model. *Bottom panel*: free gas concentration values. Dashed lines in the top and bottom panels correspond to the average gas hydrate and free gas concentrations respectively.

Preprints (www.preprints.org) | NOT PEER-REVIEWED | Posted: 26 October 2018 doi:10.20944/preprints201810.0619.v1

Peer-reviewed version available at Geosciences 2019, 9, 28; doi:10.3390/geosciences9010028

3.4 Geothermal gradient and heat flow

A variable geothermal gradient was identified, whose values range between 35 to 190 °C/km (Fig. 5). The geothermal gradient increases westernwards, reaching maximum values in correspondence of western part (at 2200 m water depth; Fig. 3), while the minimum values are located eastwards in correspondence of a water depth ranging from 600 to 1000 m. Note, that from 6 to 21 km of distance (Fig. 5) it is possible identify peaks of high values equal to 125 and 170 °C/km at 9 and 14 km of distance respectively. Moreover, a similar trend is recognized for the heat flow, showing high values equal to about 300 mWm^{-2} and located close to trench (see Fig. 2). Low values (about 100 mW/m^{-2}) are recorded upwards (see Fig. 2).

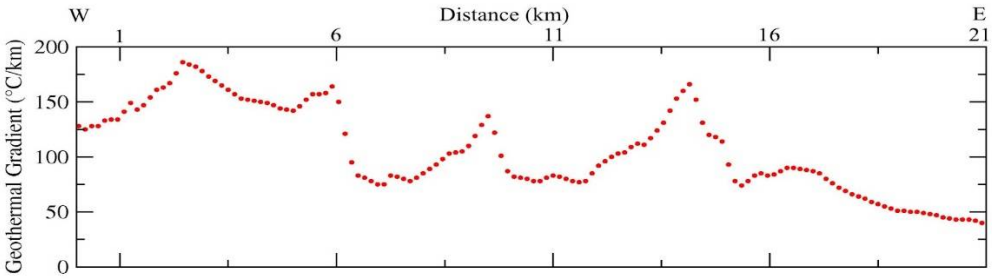

Figure 5. Geothermal gradient estimated by using BSR depth along the seismic section. See text for details.

3.5 Gas hydrate and free gas volume at standard temperature and pressure Conditions

In order to estimate the amount of methane stored in the marine sediments close to the CTJ region, bulk estimate at standard temperature and pressure (STP) conditions of hydrate and free gas concentrations were calculated using the following values:

- For gas hydrate: 4% of the total volume (dashed line in the upper panel of Fig. 4) at 50% porosity, gas hydrate layer thicknesses 108 m and a total projected area of about 2,300 km^2. Considering these assumptions, methane budget is $7.21x10^{11}$ m^3 at STP conditions.

- For free gas: 0.27% of the total volume (dashed line in the lower section of Fig. 4) at 50% porosity, free gas layer thicknesses 85 m and a total projected area of about 2,300 km^2. Considering these assumptions, methane budget just from hydrates is $4.1x10^{10}$ m^3 at STP conditions. The free gas-volume expansion ratio was calculated using the Peng-Robinson equation of state [72], applying the methodology explained by [73]. Here, we assume that free gas is composed only by methane and it is located just below the gas hydrate stability zone. We divided the area containing free gas into five sub-areas to better assess the in-situ geothermal and pressure conditions and variations of the volume expansion ratios. Table 1, shows the free gas volume at *in-situ* and STP.

Table 1. Free gas volume at *in-situ* and STP.

Interval (mbsl)	Area (m^2)	Temp. (K)	Press.(MPa)	Vol. in-situ (m^3)	Vol. STP (m^3)	Vol. exp. ratio
500-1000	4.19E+08	285.8	7.6	4.25E+07	3.69E+09	86.8
1000-1500	4.37E+08	289.7	12.7	4.44E+07	6.71E+09	151.2
1500-2000	5.59E+08	291.0	17.7	5.68E+07	1.20E+10	212.2
2000-2500	3.69E+08	291.5	22.8	3.75E+07	9.90E+09	263.9
2500-3000	2.79E+08	292.1	27.9	2.84E+07	8.67E+09	305.5
Total	**2.06E+09**			**2.10E+08**	**4.10E+10**	

Free gas volume expansion rate were calculated to estimate the volume of free gas content at STP conditions. The area was subdivided in 5 different regions, where pressure and temperature, according the corresponding geothermal gradient, were calculated.

4. Discussion

An active tectonic domain is recognisable in the seismic section; in fact, a large normal fault zone located at 7 km of distance (Fig. 3) represents the boundary between a western and eastern sector (lower and uplift part in the Fig.3, respectively). Here, the morphological features can be associated with active tectonic extension and uplift processes above the subducting CR seafloor spreading centre [39]. Further upslope deformation is characterised by normal faults and fractures with small offsets affecting shallow sediments (Fig. 3). The weak seismic character of BSR in the seaward (westward sector) is related to low free gas concentrations, while in the uplifted landward (eastward sector) a continuous and strong BSR can be related to high free gas concentrations up to 0.8% (Fig. 4). These values are consistent with free gas concentrations reported by [11] along Seismic Line 745, located northward of this study area. A shallow BSR depth with an average of 100 mbsf can be explained by high heat flow (average > 200 mW/m^2) and geothermal gradient (average ~90°C/km) as reported by [26] and in agreement with this study. Moreover, the vertical and lateral velocity variations above and below the BSR are associated to gas hydrate and free gas presence and variable concentrations respectively. In this case, the maximum velocity values above the BSR (up to 1740 m/s) correspond to high gas hydrate concentrations, whereas low velocities below the BSR (around 1290 m/s) are related to high free gas concentrations (Figs. 3 and 4).

The gas-phase concentration distribution is in general agreement with heat flow reported by [26]. An inverse correlation between gas-phase concentrations and heat flow and geothermal gradient can be recognised. Low gas hydrate and free gas concentrations coincide with high values of heat flow and geothermal gradients close to the Chile Trench and the plate boundary (Figs. 2 and 5), while high gas hydrate and free gas concentrations are associated with low heat flow and geothermal gradient further up the continental slope. A similar relationship was also recognised by [22] on the continental slope further northward at 44°S.

The observation that both gas hydrate and free gas concentrations in the sediments are lower close to the trench in the CTJ area, may be tentatively explained as a result of gas hydrate dissociation in a regime of fluid advection under high heat flow conditions. High heat flow is caused by the subduction of the Chile Rise [11,26,57,59,60], and geothermal fluids are supplied from deeper strata [67] that are undergoing deformation, anomalous compaction and de-watering (e.g. [55,65]). The highest values of heat flow are located close to the heat source near the trench (Fig. 2 and 5). Advective heat transfer in a regime of rising heat flow can change the pressure-temperature conditions, causing gas hydrate dissociation in the pore space of sediments, and the consequent increase of the free gas layer thickness below the BSR. However, active faulting and fracture in in the lower forearc will destroy stratigraphic seals and, consequently, impede free gas storage (e.g., [26,43]) above the subducting spreading ridge. Thus, gas hydrate and free gas layers close to the trench contain low concentrations, while the highest concentrations are found in shallower water depth areas where heat flow is lower, and deformation is less prevalent (Fig. 3 and 4). Note, however, that lower gas hydrate and free gas concentrations are found also near faults and fractures as expected allow to enhance fluid-escape (Fig. 3 and 4). Therefore, high heat flow due to spreading ridge subduction, tectonic faulting, and vigorous fluid advection at the leading edge of the overriding South American plate are the main controlling factors for hydrate and gas reservoir distribution offshore Taitao Peninsula.

The anomalous heat flow close to the CTJ, induced by the subduction of the young CR, alter the stable PT conditions for gas hydrate, which promotes its dissociation and fluid escapes. The dissolved methane from gas hydrates could enters into the ocean in the ventings fluid or as gas bubbles [74]. Some of the dissolved methane is diluted and oxidized as it rises through ocean interior. However,

an increase in gas methane entering the ocean above seawater saturation could lead methane to reach the ocean surface mixed layer and be transported to the atmosphere via sea-air exchange [75].

In the seepage area documented by [29], named Concepcion Methane Seep Area (CMSA, at 1,000 m water depth) high methane concentrations in seawater were recorded in correspondence with fractures, showing concentrations ~8 nM at 55 m water depth and 56 nM at 203 m water depth. This suggests that the released methane could reach the atmosphere. In comparison with the CMSA methane concentration and location, our study shows a high free gas volume estimated trapped in shallow sediments (~600 m water depth). Therefore, it is feasible to argue that portion of the stored methane in the CTJ could be transferred to the atmosphere as well contributing to global warming.

Finally, it is worth to mention that gas hydrate volume estimates are lower than other regions, e.g. offshore Patagonia [27]. We could explain these results due to: a) the shortening of the wedge (few sediment accumulation in the prism), b) faults and fractures that promote fluid and gas migration, preventing gas hydrate formation, and c) anomalous thermal state in the marine sediments that alters the gas hydrates stability zone favouring gas hydrate dissociation processes.

5. Conclusions

The results of this research for gas hydrate in the margin close to the Chile Triple Junction lead us to conclude that:

- Gas hydrate concentration values are lower than 10% of the total rock volume. The highest concentrations are found in shallower water depth areas where heat flow is lower, and deformation is less prevalent.
- Large amount of hydrate and free gas was estimated over the studied area (7.21×10^{11} m^3 and 4.1×10^{10} m^3, respectively).
- It is recognised an inverse correlation between gas-phase concentrations and heat flow and geothermal gradient. Low gas hydrate and free gas concentrations coincide with high values of heat flow and geothermal gradients over the studied area.
- An extremely high geothermal gradient was calculated, reaching values up to 190 $°Ckm^{-1}$ (caused by the subduction of the CR at the CTJ) altering the stable PT conditions for gas hydrate, which promotes its dissociation and fluid escapes.
- High heat flow, tectonic faulting, and vigorous fluid advection are the main controlling factors for hydrate and gas reservoir distribution offshore Taitao Peninsula.
- Because of the high free gas volume estimated trapped in shallow sediments (~600 m water depth), it is feasible to argue that the released methane could reach the atmosphere as well contributing to global warming.
- CTJ is an important methane seepage and should be the focus of novel geological and ecological research.

Author Contributions: Conceptualization, Lucia Villar-Muñoz and Ivan Vargas-Cordero; formal analysis, Lucia Villar-Muñoz and Ivan Vargas-Cordero; funding acquisition, Ivan Vargas-Cordero; investigation, Lucia Villar-Muñoz and Ivan Vargas-Cordero; methodology, Lucia Villar-Muñoz, Ivan Vargas-Cordero, Joaquim P. Bento, Umberta Tinivella, Francisco Fernandoy, Michela Giustiniani and Sergio Calderon; software, Lucia Villar-Muñoz, Ivan Vargas-Cordero, Joaquim P. Bento and Umberta Tinivella; supervision, Jan H. Behrmann; visualization, Lucia Villar-Muñoz and Joaquim P. Bento; writing – original draft, Lucia Villar-Muñoz; writing – review & editing, Ivan Vargas-Cordero, Joaquim P. Bento, Umberta Tinivella, Francisco Fernandoy, Michela Giustiniani, Jan H. Behrmann and Sergio Calderon.

Funding: This research was funded by CONICYT- Fondecyt de Iniciación, grant number.

Acknowledgments: Special thanks are due to Steven Cande and Stephen Lewis, who acquired the openly available data (http://www.ig.utexas.edu/) of R/V Robert Conrad Cruise RC2902. Lucía Villar-Muñoz acknowledges tenure of a DAAD scholarship for her postgraduate research and is grateful to the founders of GMT (Wessel and Smith).

Conflicts of Interest: The authors declare no conflict of interest. The funders had no role in the design of the study; in the collection, analyses, or interpretation of data; in the writing of the manuscript, or in the decision to publish the results.

References

1. Sloan, E.D. Fundamental principles and applications of natural gas hydrates. Nature. 2003, 426, 353-363.

2. Sloan, E.D.; Koh, C. Clathrate Hydrates of Natural Gases (3rd ed.). CRC Press. 2007, 752.

3. Schmidt, M.; Hensen, C.; Morz, T.; Müller, C.; Grevemeyer, I.; Wallmann, K.; Mau, S.; Kaul, N. Methane hydrate accumulation in Mound 11 mud volcano, Costa Rica forearc, Marine Geology. 2005, 216, 77-94.

4. Sloan, E.D. Clathrate Hydrates of Natural Gases (2nd ed.). CRC Press. 1998, 705.

5. Milkov, A.V. Global estimates of hydrate-bound gas in marine sediments: how much is really out there? Earth-Sci Rev. 2004, 66, 183-197.

6. Crutchley, G.J.; Mountjoy, J.J.; Pecher, I.A.; Gorman, A.R.; Henrys, S.A. Submarine Slope Instabilities Coincident with Shallow Gas Hydrate Systems: Insights from New Zealand Examples. In: Lamarche G. et al. (eds) Submarine Mass Movements and their Consequences. Advances in Natural and Technological Hazards Research. 2016, 41. Springer, Cham.

7. Hovland, M.; Orange, D.; Bjorkum, P.A.; Gudmestad, O.T. Gas hydrate and seeps-effects on slope stability: the "hydraulic model". In: The Eleventh International Offshore and Polar Engineering Conference. International Society of Offshore and Polar Engineers. 2001, 1, 471-476.

8. Kretschmer, K.; Biastoch, A.; Rüpke, L.; Burwicz, E. Modeling the fate of methane hydrates under global warming. Glob. Biogeochem. Cycles. 2015, 29(5), 610-625. doi:10.1002/2014GB005011.

9. Mountjoy, J.J.; Pecher, I.; Henrys, S.; Crutchley, G.; Barnes, P. M.; Plaza-Faverola, A. Shallow methane hydrate system controls ongoing, downslope sediment transport in a low-velocity active submarine landslide complex, Hikurangi Margin, New Zealand, Geochem. Geophys. Geosyst. 2014, 15, 4137-4156, doi:10.1002/2014GC005379.

10. Ruppel, C.D.; Kessler, J.D. The interaction of climate change and methane hydrates. Rev. Geophys. 2017, 55, 126-168. doi:10.1002/2016RG000534.

11. Bangs, N.L.; Sawyer, D.S.; Golovchenko, X. Free gas at the base of the gas hydrate zone in the vicinity of the Chile triple Junction. Geology. 1993, 21, 905-908.

12. Hyndman, R.D.; Spence, G.D. A seismic study of methane hydrate marine bottom-simulating-reflectors. J. Geophys. Res. 1992, 97, 6683-6698.

13. Kvenvolden, K.A. Comparison of marine gas hydrates in sediments of an active and passive continental margin, Mar. Petrol. Geo. 1985, 2, 65-70.

14. Vargas-Cordero, I.; Tinivella, U.; Accaino, F.; Loreto, M.F.; Fanucci, F.; Reichert, C. Analyses of bottom simulating reflections offshore Arauco and Coyhaique (Chile). Geo-Mar. Lett. 2010, 30, 271-281.

15. Brown, K.M.; Bangs, N.L.; Froelich, P.N.; Kvenvolden, K.A. The nature, distribution, and origin of gas hydrate in the Chile Triple Junction region. Earth Planet. Sci. Lett. 1996, 139, 471-483.

16. Grevemeyer, I.; Kaul, N.; Díaz-Naveas, J.L. Geothermal evidence for fluid flow through the gas hydrate stability field off Central Chile-transient flow related to large subduction zone earthquakes? Geophys. J. Int. 2006, 166, 461-468.

17. Loreto, M.F.; Tinivella, U.; Ranero, C. Evidence for fluid circulation, overpressure and tectonic style along the Southern Chilean margin. Tectonophysics. 2007, 429, 183-200.

18. Polonia, A.; Brancolini, G.; Torelli, L.; Vera, E. Structural variability at the active continental margin off southernmost Chile. Geodynamics. 1999, 27, 289-307.

19. Polonia, A.; Brancolini, G.; Torelli, L. The accretionary complex of southernmost Chile from the strait of Magellan to the Drake passage. Terra Antarctica. 2001, 8(2), 87-98.

20. Polonia, A.; Torelli, L. Antarctic/Scotia plate convergence off southernmost Chile. Geologica Acta. 2007, 5, 295-306.

21. Polonia, A.; Torelli, L.; Brancolini, G.; Loreto, M.F. Tectonic accretion versus erosion along the southern Chile trench: Oblique subduction and margin segmentation. Tectonics. 2007, 26, TC3005.

22. Vargas-Cordero, I.; Tinivella, U.; Accaino, F.; Loreto, M. F.; Fanucci, F. Thermal state and concentration of gas hydrate and free gas of Coyhaique, Chilean Margin (44° 30' S). Marine and Petroleum Geology. 2010, 27(5), 1148-1156.

23. Vargas-Cordero, I.; Tinivella, U.; Accaino, F.; Fanucci, F.; Loreto, M.F.; Lascano, M.E.; Reichert, C. Basal and Frontal Accretion Processes versus BSR Characteristics along the Chilean Margin. J. Geol. Res. 2011, 2011, 1-10.

24. Vargas-Cordero, I.; Tinivella, U.; Villar-Muñoz, L.; Giustiniani, M. Gas hydrate and free gas estimation from seismic analysis offshore Chiloé island (Chile). Andean Geol. 2016, 43 (10), 263-274.

25. Vargas-Cordero, I.; Tinivella, U.; Villar-Muñoz, L. Gas Hydrate and Free Gas Concentrations in Two Sites inside the Chilean Margin (Itata and Valdivia Offshores). Energies. 2017, 10(12), 2154, doi:10.3390/en10122154.

26. Villar-Muñoz, L.; Behrmann, J.H.; Diaz-Naveas, J.; Klaeschen, D.; Karstens, J. Heat flow in the southern Chile forearc controlled by large-scale tectonic processes. Geo-Mar. Lett. 2014, 34, 185-198, doi:10.1007/s00367-013-0353-z.

27. Villar-Muñoz, L.; Bento, J.P.; Klaeschen, D.; Tinivella, U.; Vargas-Cordero, I.; Behrmann, J. H. A first estimation of gas hydrates offshore Patagonia (Chile). Mar. Petrol. Geol. 2018, 96, 232-239. doi: 10.1016/j.marpetgeo.2018.06.002.

28. Coffin, R.; Pohlman, J.; Gardner, J.; Downer, R.; Wood, W.; Hamdan, L.; Walker, S.; Plummerg, R.; Gettrus, J.; Diaz J. Methane hydrate exploration on the mid Chilean coast: A geochemical and geophysical survey, J. Petrol. Sci. Eng. 2007, 56(1), 32-41.

29. Geersen, J.; Scholz, F.; Linke, P.; Schmidt, M.; Lange, D.; Behrmann, J.H.; Volker, D.; Hensen, C. Fault zone controlled seafloor methane seepage in the rupture area of the 2010 Maule earthquake, Central Chile. Geochem. Geophy. Geosy 2016, 17, 4802- 4813, doi:10.1002/2016GC006498.

30. Jessen, G.L.; Pantoja, S.; Gutierrez, M.A.; Quinones, R.A.; Gonzalez, R.R.; Sellanes, J.; Kellermann M.Y.; Hinrichs K.U. Methane in shallow cold seeps at Mocha Island off central Chile, Continental Shelf Research. 2011, 31, 574-581.

31. Sellanes, J.; Quiroga, E.; Gallardo, V. First direct evidence of methane seepage and associated chemosynthetic communities in the bathyal zone off Chile. Journal of the Marine Biological Association of the United Kingdom. 2004, 84(05), 1065-1066, doi: 10.1017/S0025315404010422h.

32. Sellanes, J.; Krylova, E. A new species of Calyptogena (Bivalvia, Vesicomyidae) from a recently discovered methane seepage area off Concepción Bay, Chile (36S). Journal of the Marine Biological Association UK. 2005, 85, 969-976.

33. Sellanes, J.; Quiroga, E.; Neira, C. Megafaunal community structure and trophic relationships of the recently discovered Concepción Methane Seep Area (Chile, 36S). ICES Journal of Marine Sciences. 2008, 65, 1102-1111.

34. Scholz, F.; Hensen, C.; Schmidt, M.; Geersen J. Submarine weathering of silicate minerals and the extent of pore water freshening at active continental margins, Geochim. Cosmochim. Acta. 2013, 100, 200-216.

35. German, C.R.; Shank, T.M.; Lilley, M.D.; Lupton, J.E.; Blackman, D.K.; Brown, K.M.; Baumberger, T.; FrühGreen, G.; Greene, R.; Saito, M.A.; Sylva, S.; Nakamura, K.; Stanway, J.; Yoerger, D.R.; Levin, L.A.; Thurber, A.R.; Sellanes, J.; Mella, M.; Muñoz, J.; Diaz-Naveas, J.L. Inspire Science Team, 2010. Hydrothermal Exploration at the Chile Triple Junction – ABE's Last Adventure? American Geophysical Union, Fall Meeting 2010. Abstract #OS11D-06.

36. Oliver, P.G.; Sellanes, J. New species of Thyasiridae from a methane seepage area off Concepción , Chile. Zootaxa. 2005, 1092, 1-20.

37. Völker, D.; Geersen, J.; Contreras-Reyes, E.; Sellanes, J.; Pantoja, S.; Rabbel, W.; Thorwart, M.; Reichert, C.; Block, M.; Weinrebe, W.R. Morphology and geology of the continental shelf and upper slope of southern Central Chile (33S–43S). Int J Earth Sci (Geol Rundsch). 2014, 103, 1765. doi:10.1007/s00531-012-0795-y.

38. Olu, K.; Duperret, A.; Sibuet, M., Foucher, J.P.; Fiala-Medioni, A. Structure and distribution of cold seep communities along the Peruvian active margin: relationship to geological and fluid patterns. Marine Ecology Progress Series. 1996, 132, 109-125.

39. Behrmann, J.H., Lewis, S.D., Cande, S.C. Tectonics and geology of spreading ridge subduction at the Chile Triple Junction: a synthesis of results from Leg 141 of the Ocean Drilling Program. Geologische Rundschau. 1994, 83(4), 832-852.

40. Hillman, J.I.T.; Klaucke, I.; Bialas, J.; Feldman, H.; Drexler, T.; Awwiller, D.; Atgin, O.; Çifçi, G. Gas migration pathways and slope failures in the Danube Fan, Black Sea. Mar. Petrol. Geol. 2018, 92, 1069-1084, doi: 10.1016/j.marpetgeo.2018.03.025.

41. Hovland, M.; Svensen, H.; Forsberg, C.F.; Johansen, H.; Fichler, C.; Fosså, J.H.; Jonsson, R.; Rueslåtten, H. Complex pockmarks with carbonate-ridges off mid-Norway: Products of sediment degassing. Mar. Geol. 2005, 218, 191-206.

42. Römer, M.; Sahling, H.; Pape, T.; Bohrmann, G.; Spieß, V. Quantification of gas bubble emissions from submarine hydrocarbon seeps at the Makran continental margin (offshore Pakistan). J. Geophys. Res. 2012, 117, C10015, doi:10.1029/2011JC007424.

43. Vargas-Cordero, I.; Tinivella, U.; Villar-Muñoz, L; Bento, J.P. High Gas Hydrate and Free Gas Concentrations: An Explanation for Seeps Offshore South Mocha Island. Energies. 2018, in press

44. Tinivella, U; Carcione, J.M. Estimation of gas-hydrate concentration and free-gas saturation from log and seismic data. The Leading Edge.. 2001, 20(2), 200-203.

45. Cisternas, M.; Atwater, B.F.; Torrejón, F.; Sawai, Y.; Machuca, G.; Lagos, M.; Eipert, A.; Youlton, C.; Salgado, I.; Kamataki, T.; Shishikura, M.; Rajendran C.P.; Malik, J.K.; Rizal, Y.; Husni, M. Predecessors of the giant 1960 Chile earthquake. Nature. 2005, 437, 404-407.

46. Agurto-Detzel, H.; Rietbrock, A.; Bataille, K.; Miller, M.; Iwamori, H.; Priestley, K. Seismicity distribution in the vicinity of the Chile Triple Junction, Aysén Region, southern Chile, Journal of South American Earth Sciences. 2014, 51, 1-11.

47. Murdie, R.E.; Prior, D.J.; Styles, P.; Flint, S.S.; Pearce, R.G.; Agar, S.M. Seismic responses to ridge-transform subduction: Chile triple junction. Geology. 1993, 21, 1095-1098.

48. Fischer, D.; Mogollón, J.M.; Strasser, M.; Pape, T.; Bohrmann, G.; Fekete, N.; Spiess, V.; Kasten, S. Subduction zone earthquake as potential trigger of submarine hydrocarbon seepage. Nat. Geosci. 2013, 6(8), 647-651.

49. Sibson, R.H. Interactions between temperature and pore fluid pressure during earthquake faulting - A mechanism for partial or total stress relief. Nature. 1973, 243, 66-68.

50. Boobalan, A.J.; Ramanujam, N. Triggering mechanism of gas hydrate dissociation and subsequent submarine landslide and ocean wide Tsunami after Great Sumatra-Andaman 2004 earthquake. Arch. Appl. Sci. Res. 2013, 5, 105-110.

51. Elger, J.; Berndt, C.; Rüpke, L.H.; Krastel, S.; Gross, F.; Geissler, W.H. Submarine slope failures due to pipe structure formation. Nat. Commun. 2018, 9,715.

52. Kvenvolden, K.A. Gas hydrates-geological perspective and global change. Rev. Geophys. 1993, 31, 173-187. doi:10.1029/93RG00268.

53. Waite, W. F.; Santamarina, J.C.; Cortes, D.D.; Dugan, B.; Espinoza, D.N.; Germaine, J.; Jang, J.; Jung, J.W.; Kneafsey, T. J.; Shin, H.; Soga, K.; Winters, W.J.; Yun, T.S. Physical properties of hydrate-bearing sediments. Rev. Geophys. 2009, 47, RG4003, doi: 10.1029/2008RG000279.

54. Xu, W.; Germanovich, L.N. Excess pore pressure resulting from methane hydrate dissociation in marine sediments: A theoretical approach. J. Geophys. Res. 2006, 111, doi:10.1029/2004JB003600.

55. Behrmann, J.H.; Lewis, S.D.; Musgrave, R.; Bangs, N.; Bodén, P.; Brown, K.; Collombat, H.; Didenko, A.N.; Didyk, B.M.; Froelich, P.N.; Golovchenko, X.; Forsythe, R.; Kurnosov, V.; Lindsley-Griffin, N.; Marsaglia, K.; Osozawa, S.; Prior, D.; Sawyer, D.; Scholl, D.; Spiegler, D.; Strand, K.; Takahashi, K.; Torres, M.; Vega-Faundez, M.; Vergara, H.; Waseda, A. Chile Triple Junction. In Proc. ODP, Init. Repts. (Pt. A). 1992, 141, 1-708.

56. Cande, S.C.; Leslie, R.B. Late Cenozoic tectonics of the southern Chile trench. J. Geophys. Res. 1986, 91, 471-496.

57. Cande, S.C.; Leslie, R.B.; Parra, J.C.; Hodbart, M. Interaction between the Chile ridge and Chile trench: Geophysical and geothermal evidences. J. Geophys. Res. 1987, 92, 495-520.

58. Herron, E.M.; Cande, S.C.; Hall, B.R. An active spreading center collides with a subduction zone: A geophysical survey of the Chile margin triple Junction. Memoirs - Geological Society of America. 1981, 154, 683-701.

59. Brown, K.M.; Bangs N.L.; Marsaglia, K.; Froleich, P.N.; Zheng, Y.; Didyk, B.M.; Prior, D.; Richford, E.L.; Torres, M.; Kumsov, V.B.; Lindsley-Grifftn, N.; Osozawa S.; Waseda, A. A summary of ODP 141 hydrogeologic, geochemical, and thermal results. Proc. ODP Sci. Results 141. 1995, 363-373.

60. Flueh and Grevemeyer. FS Sonne Fahrtbericht/cruise report SO181 TIPTEQ: from the Incoming Plate to mega Thrust EarthQuakes, Valparaíso - Talcahuano. 2005. doi:06.12.2004-26.02.2005.

61. Völker, D.; Grevemeyer, I.; Stipp, M.; Wang, K.; He, J. Thermal control of the seismogenic zone of southern central Chile, J. Geophys. Res. 2011, 116, B10305, doi: 10.1029/2011JB008247.

62. Lagabrielle, Y.; Guivel, C.; Maury, R.; Bourgois, J.; Fourcade, S.; Martin H. Magmatic-tectonic effects of high thermal regime at the site of active ridge subduction: The Chile Triple Junction model. Tectonophysics. 2000, 326, 255-268.

63. German C.R.; Ramirez-Llodra, E.; Baker, M.C.; Tyler, P.A.; ChEss Scientific Steering Committee. Deep-Water Chemosynthetic Ecosystem Research during the Census of Marine Life Decade and Beyond: A Proposed Deep-Ocean Road Map. PLoS ONE. 2011, 6(8), e23259, doi:10.1371/journal.pone.0023259.

64. Bangs, N.L.; Brown, K.M. Regional heat flow in the vicinity of the Chile Triple Junction constrained by the depth of the bottom simulating reflection, Proc. ODP, Sci. Results 141. 1995, 253-259.

65. Behrmann, J.H.; Kopf, A. Balance of tectonically accreted and subducted sediment at the Chile Triple Junction. Int. J. Earth Sciences (Geol. Rundsch.). 2001, 90, 753-768.

66. Bourgois, J.; Martin, H.; Lagabrielle, Y.; Le Moigne, J.; Frutos Jara, J. (Chile margin triple junction area) Subduction erosion related to spreading-ridge subduction: Taitao peninsula Geology. 1996, 24, 723-726.

67. Bangs, N.L.; Cande, S.C. Episodic development of a convergent margin inferred from structures and processes along the southern Chile margin. Tectonics. 1997, 16(3), 489-503, doi: 10.1029/97TC00494.

68. Cohen, J.K.; Stockwell, J.W. CWP/SU: Seismic Unix Release 4.0: A free Package for Seismic Research and Processing, Center for Wave Phenomena, Colorado School of Mines: Golden, CO, USA. 2008, 1-153.

69. Loreto, M.F.; Tinivella, U.; Accaino, F.; Giustiniani, M. Offshore Antarctic Peninsula gas hydrate reservoir characterization by geophysical data analysis. Energies. 2011, 4(1), 39-56.

70. Yilmaz, O. Seismic Data Analysis: Processing, Inversion and Interpretation of Seismic Data. 2nd Edition. Society of Exploration Geophysicists, Oklahoma. 2001, 2027.

71. Liu, Z.; Bleistein, N. Migration velocity analysis: Theory and an iterative algorithm. Geophysics. 1995, 60, 142-153.

72. Peng, D.; Robinson, D.B. A new two-constant equation of state. Industrial and Engineering Chemistry Fundamentals. 1976, 15(1), 59-64. doi:10.1021/i160057a011

73. Barth, Ginger. Methane Gas Volume Expansion Ratios and Ideal Gas Deviation Factors for the Deep Water Bering Sea Basins. USGS Open-File Report. 2005,1451.

74. Reeburgh, W. S. Oceanic Methane Biogeochemistry. Chem. Rev. 2007, 107, 486-513.

75. Cynar, F. J. & Yayanos, A. A. In: Oremland, R. S. (eds) Biogeochemistry of Global Change: Radiatively Active Trace Gases. 1993, 551–573. Chapman-Hall